



TUMORIGENESIS AND NEOPLASTIC PROGRESSION

Specific Polo-Like Kinase 1 Expression in Nodular Lymphocyte-Predominant Hodgkin Lymphoma Suggests an Intact Immune Surveillance Program



Jonathan Weiss,^{*} Kathryn Gibbons,[†] Vida Ehyae,[‡] Vanessa Perez-Silos,[§] Alejandro Zevallos,[§] Mark Maienschein-Cline,[¶] Eileen Brister,^{||} Maria Sverdlow,^{||} Eshana Shah,^{**} Jayalakshmi Balakrishna,^{††} Emily Symes,^{‡‡} John K. Frederiksen,[§] Peter H. Gann,[§] Robert Post,[§] Nicolas Lopez-Hisijos,[‡] John Reneau,^{§§} Girish Venkataraman,^{‡‡} Nathanael Bailey,^{¶¶} Noah A. Brown,^{|||} Mina L. Xu,^{***} Ryan A. Wilcox,^{*} Kedar Inamdar,[†] and Carlos Murga-Zamalloa[§]

From the Departments of Internal Medicine* and Pathology,^{|||} University of Michigan, Ann Arbor, Michigan; the Department of Pathology,[†] Henry Ford Hospital, Detroit, Michigan; the Department of Pathology,[‡] Rush University, Chicago, Illinois; the Departments of Pathology[§] and Internal Medicine,^{**} the Research Informatics Core,[¶] and the Research Tissue Imaging Core and Research Histology Core,^{||} University of Illinois at Chicago, Chicago, Illinois; the Departments of Pathology^{††} and Internal Medicine,^{§§} Ohio State University, Columbus, Ohio; the Department of Pathology,^{‡‡} University of Chicago, Chicago, Illinois; the Department of Pathology,^{¶¶} University of Pittsburgh Medical Center, Pittsburgh, Pennsylvania; and the Department of Pathology,^{***} Yale University, New Haven, Connecticut

Accepted for publication
October 18, 2023.

Address correspondence to
Kedar Inamdar, M.D., Department of Pathology, Henry Ford Health, 2799 W. Grand Blvd., Detroit, MI 48202; or Carlos Murga-Zamalloa, M.D., Department of Pathology, University of Illinois at Chicago, 840 S. Wood St., 230 CMET, Chicago, IL 60605.
E-mail: kinamdal@hfhs.org or catto@uic.edu.

Nodular lymphocyte-predominant Hodgkin lymphoma (NLPHL) is a rare and relatively indolent B-cell lymphoma. Characteristically, the [lymphocyte-predominant (LP)] tumor cells are embedded in a microenvironment enriched in lymphocytes. More aggressive variants of mature B-cell and peripheral T-cell lymphomas exhibit nuclear expression of the polo-like kinase 1 (PLK1) protein, stabilizing MYC (alias c-myc) and associated with worse clinical outcomes. This study demonstrated expression of PLK1 in the LP cells in 100% of NLPHL cases ($n = 76$). In contrast, <5% of classic Hodgkin lymphoma cases ($n = 70$) showed PLK1 expression within the tumor cells. Loss-of-function approaches demonstrated that the expression of PLK1 promoted cell proliferation and increased MYC stability in NLPHL cell lines. Correlation with clinical parameters revealed that the increased expression of PLK1 was associated with advanced-stage disease in patients with NLPHL. A multiplex immunofluorescence panel coupled with artificial intelligence algorithms was used to correlate the composition of the tumor microenvironment with the proliferative stage of LP cells. The results showed that LP cells with PLK1 (high) expression were associated with increased numbers of cytotoxic and T-regulatory T cells. Overall, the findings demonstrate that PLK1 signaling increases NLPHL proliferation and constitutes a potential vulnerability that can be targeted with PLK1 inhibitors. An active immune surveillance program in NLPHL may be a critical mechanism limiting PLK1-dependent tumor growth. (*Am J Pathol* 2024, 194: 165–178; <https://doi.org/10.1016/j.ajpath.2023.10.008>)

Nodular lymphocyte-predominant Hodgkin lymphoma (NLPHL) is a rare subtype of mature B-cell lymphoma that accounts for <5% of B-cell lymphoma cases. NLPHL is characterized by an indolent clinical course, with overall survival rates >90% after 10 years of diagnosis.^{1–3} The relapse rates are higher than classic Hodgkin lymphoma and range from 15% to 20% over 8 to 10 years.⁴ Transformation

to aggressive lymphoma subtypes is uncommon and occurs in approximately 2% to 8% of the cases.⁵ The current management strategies are variable and include

Supported by the American Society of Hematology—Harold Amos Medical Faculty Development Program award (C.M.-Z.).
K.I. and C.M.-Z. contributed equally to this work.

immunochemotherapy, radiotherapy, and watchful waiting in patients with asymptomatic and nonbulky disease.^{6,7}

Morphologically, NLPHL is characterized by large, atypical lymphocytes with convoluted nuclei [lymphocyte-predominant (LP) cells], set within a background of numerous small lymphocytes.⁸ Rosettes of T-follicular helper (T_{FH}) type T cells immediately surround the LP cells, which comprise <5% of total cells.⁹ In contrast to classic Hodgkin lymphoma (cHL), the tumor cells of NLPHL characteristically express B-cell markers and are usually negative for CD30 expression. However, LP cells may occasionally express CD30 and/or CD15, making the distinction between NLPHL and cHL challenging.^{10,11} The histologic distinction between NLPHL and T-cell/histiocyte-rich large B-cell lymphoma (THRLBCL), an aggressive B-cell lymphoma variant, also poses difficulties. These arise because one variant morphologic pattern of NLPHL (pattern E) is indistinguishable from THRLBCL, and the neoplastic cells of NLPHL and THRLBCL express a similar immunophenotype.^{11–15} Sometimes, NLPHL may mimic reactive conditions, such as progressive transformation of germinal centers, particularly when limited tissue is available for diagnosis.

The tumor microenvironment of NLPHL is predominantly composed of T cells with a variable number of background B-cell lymphocytes.⁹ In contrast to reactive lymphoid tissue, increased programmed cell death 1 (PD1)⁺CD4⁺ T-cell subsets have been detected in NLPHL cases, and T_{FH} type lymphocytes provide an advantage for LP cell survival via direct paracrine stimulation of IL21 receptor.¹⁶ In addition, the presence of forkhead box P3 (FoxP3)⁺CD4⁺ T-regulatory cells (T-regs) could modulate the number of T_{FH} cells in the immediate proximity of LP cells,⁹ further sustaining the survival and growth of the tumor component.

The polo-like kinase 1 (PLK1) protein is a serine/threonine kinase that promotes cell cycle progression and proliferation.¹⁷ PLK1 increases the protein stability of MYC (alias c-myc) oncoprotein by preventing its degradation by the ubiquitin-proteasome pathway. Increased expression of PLK1 has been detected in aggressive B- and T-cell lymphomas, and this directly correlates with the expression of MYC in high-grade B-cell lymphomas.¹⁸ In contrast, the expression of PLK1 is not detected in small B-cell lymphomas, including follicular lymphoma, mantle cell lymphoma, and small lymphocytic lymphoma.¹⁸ Therefore, the expression of PLK1 was evaluated in NLPHL cases to delineate further its diagnostic utility of discriminating NLPHL (particularly the variant histologic patterns) from aggressive counterparts.

Materials and Methods

Reagents

Reagents used for these studies included antibodies for Western blot analysis, MYC, PLK1, and glyceraldehyde-3-

phosphate dehydrogenase (Cell Signaling Technologies, Danvers, MA). Proliferation assays were performed using CellTiter Glo (Promega, Madison, WI) reagent, per the manufacturer's instructions. Volasertib was purchased from Selleckchem (Houston, TX). Reagents used for immunohistochemistry and immunofluorescence are detailed in upcoming sections.

Tumor Samples

A retrospective cohort of 76 NLPHL cases was collected from the pathology archives of the University of Illinois at Chicago, University of Chicago (Chicago, IL), Yale University (New Haven, CT), Henry Ford Hospital (Detroit, MI), University of Pittsburgh (Pittsburgh, PA), Rush University (Chicago, IL), Ohio State University (Columbus, OH), and the University of Michigan (Ann Arbor, MI). Hematoxylin and eosin sections, CD20 immunostainings, and PLK1 immunostainings were centrally reviewed by two pathologists (K.I. and C.M.-Z.). All the clinical data were annotated in JMP Clinical software version 7.1 (JMP Statistical Discovery, LLC, Cary, NC). A retrospective cohort of 70 cases of classic Hodgkin lymphoma was obtained from Henry Ford Hospital, the University of Illinois at Chicago, and the University of Michigan. This study was performed with the approval of the Institutional Review Board of the University of Illinois at Chicago (STUDY2022-0757).

Immunohistochemistry

All slides were deparaffinized and stained on BOND RX autostainer (Leica Microsystems, Wetzlar, Germany). For single chromogen PLK1 staining, slides were subjected to antigen retrieval with BOND Epitope Retrieval solutions 2 (Leica Microsystem; number AR9640) for 20 minutes at 99°C and stained using BOND Polymer Refine Detection kit (Leica Microsystems; number DS9800). The non-specific signal was blocked by incubating the slides with peroxide block for 15 minutes and protein block (Background Sniper; Biocare Medical, Pacheco, CA; number BS966) for 15 minutes at room temperature. Slides were stained with anti-PLK1 rabbit monoclonal antibody (1:50; Cell Signaling, Danvers, MA; number 4531) for 30 minutes, and the signal was detected with polymer—horseradish peroxidase/diaminobenzidine. Slides were counterstained with hematoxylin, dehydrated on Autostainer XL (Leica Microsystems), and mounted with Micromount (Leica Microsystems; number 3801730). For dual sequential PLK1 and CD30 staining, samples were stained with PLK1, as described above, without the hematoxylin counterstain, followed by staining with anti-CD30 ready-to-use mouse monoclonal antibody (Millipore-Sigma, Burlington, MA; number 130M-98) and BOND Polymer Refine Red Detection Kit (Leica Microsystems; number DS9390). Incubation with CD30 antibodies was for 30 minutes, and the signal

was developed with Polymer-AP and Fast Red (Leica Microsystems).

For multiplex immunofluorescence (mIF), a panel consisting of CD3, CD4, CD20, PD1, PLK1, FoxP3, and DAPI was optimized on tonsil and lymphoma samples using BOND RX autostainer and BOND Research Detection System (Leica Microsystems; number DS9455). Opal 6-plex Detection Kit (Akoya Biosciences, Marlborough, MA; number NEL821001KT) was used for detection. For previously optimized targets, monoplex staining slides at the assigned position and with the assigned Opal dye were prepared for each target and spectrally unmixed. The staining patterns were compared with the single chromogen immunohistochemistry performed on the adjacent slide, and the intensity of the signal was also assessed for each target to ensure it was in the desired range. For PLK1, PD1, and CD20, additional optimization steps, such as serial dilutions, testing of different positions in the multiplex sequence, and stripping controls, were performed to ensure the optimal staining conditions and complete removal of the primary and secondary antibodies after each round of staining. The final multiplex panel information is listed in [Table 1](#). Dual antigen retrieval with BOND Epitope Retrieval Buffers 1 and 2 (Leica Microsystems) was performed before the beginning of the staining protocol. BOND Epitope Retrieval Buffer 1 was used for stripping primary and secondary antibodies after each staining round.

Multiplex Immunofluorescence Imaging

Slides were scanned using a PhenoImager HT multispectral microscope (Akoya Biosciences) in multispectral images mode at 20× resolution. Regions of interest containing tumor cells were manually selected by a pathologist (C.M.-Z. or R.P.) and scanned at 40× resolution. Spectral profiles were optimized using Nuance software version 3.0 (Akoya Biosciences) to ensure the accurate unmixing of each multispectral channel. Multispectral images were analyzed using HALO software version 3.5 (Indica Labs, Albuquerque, NM) and custom-written MATLAB code. A pathologist (C.M.-Z. or R.P.) manually annotated tumor (LP cell) cells. Quantifying tumor cell PLK1 intensity was performed using Halo Area Quantification FI Module version 2.3.3. The tumor cell nucleus was defined as the region negative for CD20. The

tumor cell cytoplasm was defined as the positive region for CD20. The mean PLK1 intensity was reported for the nucleus, cytoplasm, and whole cell for each annotation region. Images were manually annotated to outline tissue regions and remove artifacts. Nuclear segmentation was performed using a manually trained HALO AI Nuclei Seg classifier (Indica Labs). HALO HighPlex FL module version 4.1.3 (Indica Labs) was used to manually set thresholds for each channel and manually identify cell phenotypes. Cell phenotypes and position coordinates were exported from HALO for spatial analysis. Spatial analysis identifying the immune cells within each tumor microenvironment was performed in MATLAB. The mean width of all immune cells was calculated to be 7.89 μm. The average width of five cells was estimated to be 40 μm. For each tumor cell, the tumor microenvironment was defined as an 80- by 80-μm square with the same center as the tumor cell annotation, excluding the tumor cell annotation region. All immune cells within the tumor microenvironment were identified for each tumor cell.

Statistical Analysis

Comparisons of PLK1 expression and tumor microenvironment were conducted in R version 4.3 (<https://www.r-project.org>). Tumor PLK1 expression levels were binned to either high or low levels based on a threshold of 8. This threshold was determined by inspection of density plots of PLK1 levels over the data set: the mean level of PLK1 varied from subject to subject, and threshold 8 was determined to be an effective separator of the high and lower distributions. In addition, a value of 8 was close to the median for the data set over all subjects, providing an even split of PLK1 levels. On the basis of the distribution of %PLK1^{high} LP cells in all the cases, a threshold of 20% of PLK1^{high} tumor cells was determined to be in the middle. Therefore, the cases were dichotomized in predominant PLK1^{high} (>20% of PLK1^{high} LP cells) or not. This was done to correlate with the limited or advanced clinical stage and variant patterns.

For each immune cell type, the fraction of immune cells were counted in the microenvironment of PLK1 high or low tumor cells. The overall number of PLK1 high or low tumor cells were also counted and a log2 odds ratio was computed for each immune cell *i* as follows:

Table 1 List of Antibodies Used for Multiplex Imaging and Immunohistochemistry Analysis

Order	Target	Antibody, manufacturer, catalog no.	Dilution	Opal dye	Opal dye dilution
1	PD1	Cell Signaling, 43248	1:100	620	1:150
2	PLK1	Cell Signaling, 4513	1:50	650	1:150
3	CD3	Abcam (Cambridge, UK), 16669	1:100	690	1:100
4	FoxP3	Cell Signaling, 12653	1:100	570	1:150
5	CD4	Millipore-Sigma, 104R	1:100	520	1:100
6	CD20	Leica Biosystems, CD20-L26-L-CE	1:1000	540	1:150

FoxP3, forkhead box P3; PD1, programmed cell death 1; PLK1, polo-like kinase 1.

$$\log 2OR_i = \log 2 \left(\frac{PLK1_{high_i}/PLK1_{low_i}}{PLK1_{high_{all}}/PLK1_{low_{all}}} \right) \quad (1)$$

Where $PLK1_{high_i}$ and $PLK1_{low_i}$ are the fraction of immune cell i in the microenvironment of PLK1 high or low tumor cells, $PLK1_{high_{overall}}$ and $PLK1_{low_{overall}}$ are the overall fraction of PLK1 high or low tumor cells, and $\log 2OR_i$ is the log2 odds ratio for immune cell i .

These statistics were computed in aggregate over all samples. However, high variability in both PLK1 levels and immune cell types from sample to sample was identified. Bootstrapping was used to compute CIs for the above statistics to quantify the uncertainty in the estimates due to this variability. The study sampled 20 times, with replacement, from the original grouping of 20 samples and computed $PLK1_{high_{overall}}$, $PLK1_{low_{overall}}$, plus $PLK1_{high_i}$, $PLK1_{low_i}$, and $\log 2OR_i$ for each immune cell type. This process was repeated 1000 times and 95% CIs were obtained for each statistic as the 2.5 to 97.5 percentiles over all bootstraps. P values were computed from the CIs for the log2 odds ratios, as described by Altman and Bland.¹⁹ Q values were computed by adjusting P values for multiple testing using the false discovery rate procedure over all the immune cells tested.

Ethical Approval and Consent to Participate

This study was performed with the approval of the Institutional Review Board of the University of Illinois at Chicago (STUDY2022-0757). The study was performed in accordance with the Declaration of Helsinki.

Results

PLK1 Expression Is Detected in NLPHL Tumor Cells

The expression of the PLK1 protein was evaluated by immunohistochemistry in a cohort of NLPHL cases and reactive lymphoid tissue obtained from eight different institutions. Native expression of PLK1 occurred predominantly within germinal center lymphocytes in benign reactive lymphoid tissues (Figure 1). Interestingly, PLK1 expression was detected in at least 10% of the LP cells in all the NLPHL cases evaluated ($n = 76$) (Figure 1), and the average percentage of PLK1-positive LP cells was 68% (range, 10% to $\geq 95\%$) (Figure 2 and Supplemental Figure S1). PLK1 expression was detected in both the cytoplasmic and nuclear compartments of the LP cells, and at variable intensity (Figure 1). This was in contrast to aggressive B- and T-cell

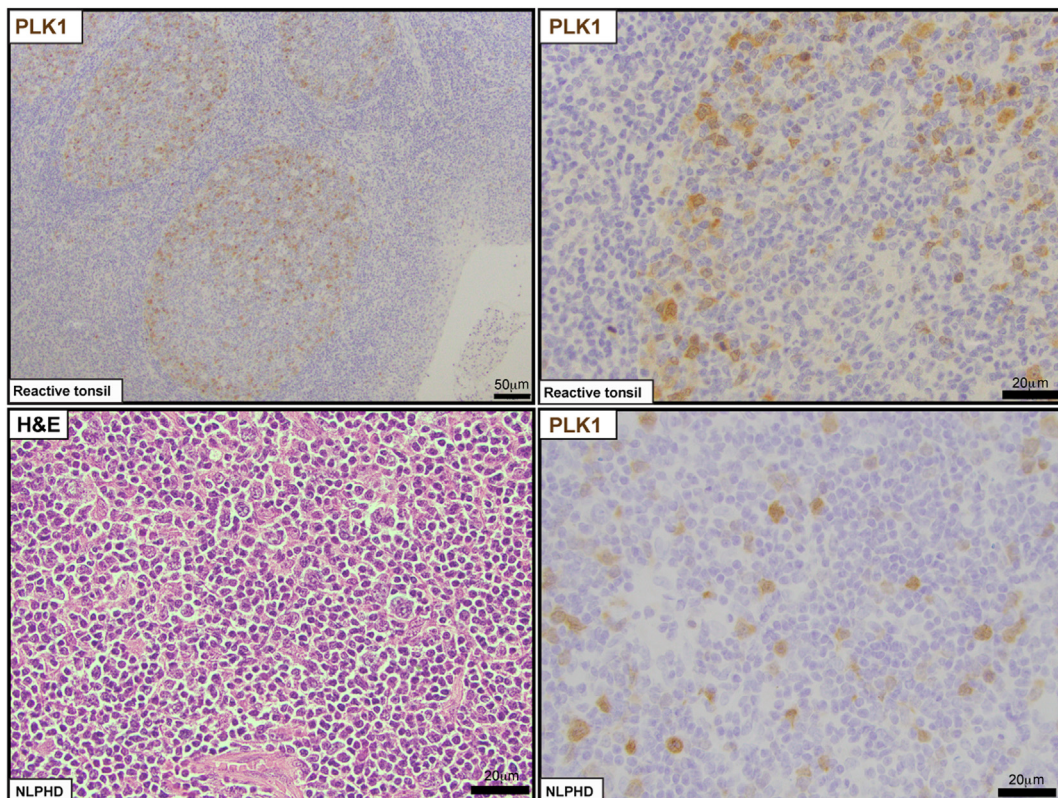


Figure 1 Polo-like kinase 1 (PLK1) expression in nodular lymphocyte-predominant Hodgkin lymphoma (NLPHL) tumor cells. **Top panels:** Evaluation of PLK1 expression in reactive tonsils occurs predominantly within germinal center lymphocytes. **Bottom panels:** PLK1 expression is detected in lymphocyte-predominant cells in NLPHL within the cytoplasm and nuclear compartments at variable intensities. Scale bars: 50 μm (top left panel); 20 μm (top right panel and bottom panels). H&E, hematoxylin and eosin.

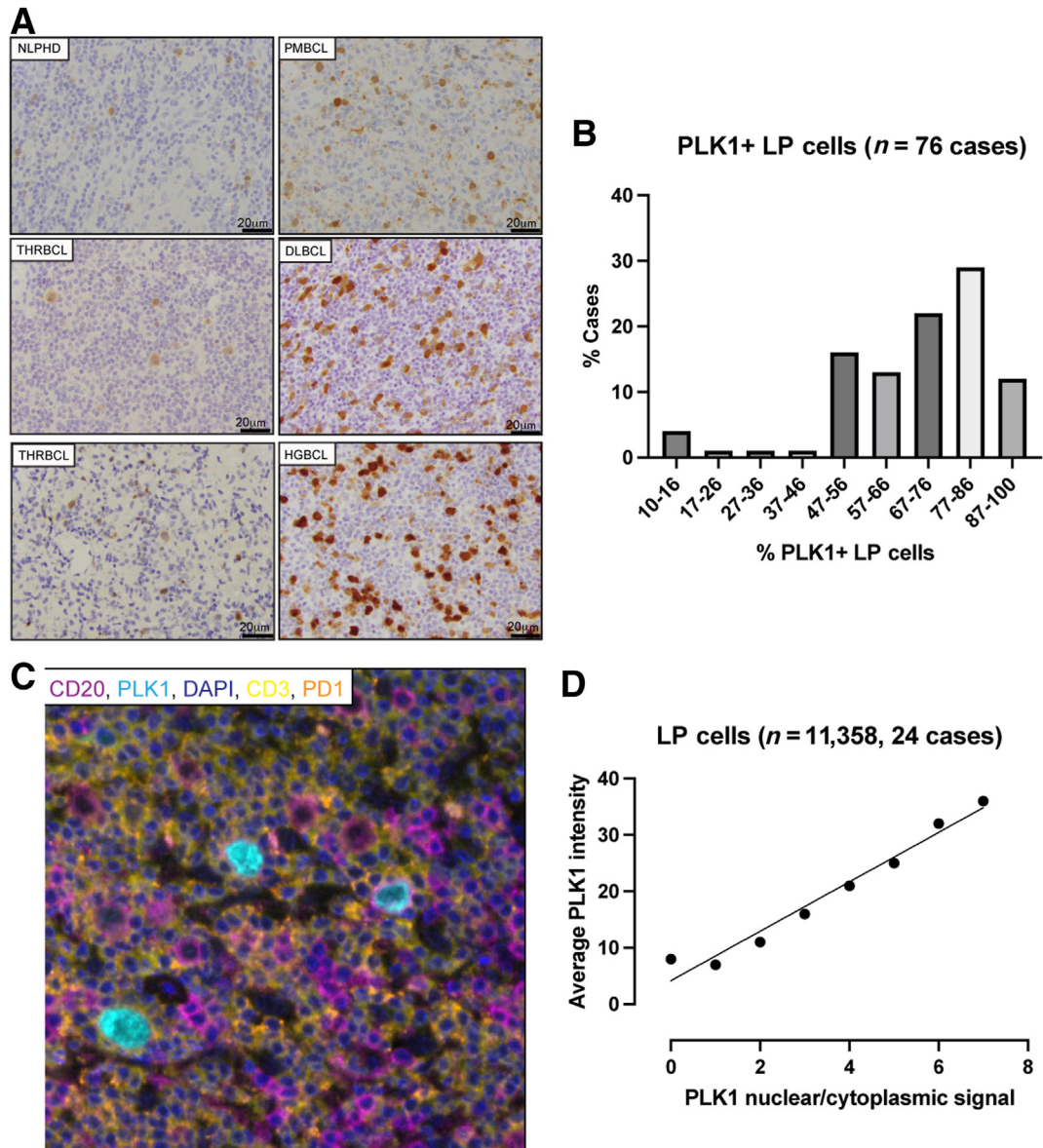


Figure 2 Polo-like kinase 1 (PLK1) expression in lymphocyte-predominant (LP) cells. **A:** PLK1 expression in nodular lymphocyte-predominant Hodgkin lymphoma (NLPHL) compared with aggressive B-cell lymphomas. **B:** Distribution of cases and the percentage of LP cells with positive expression for PLK1. **C:** Multiplex immunofluorescence imaging demonstrates positive expression of PLK1 in LP cells surrounded by CD3/programmed cell death 1 (PD1)-positive T-cell lymphocytes. **D:** Graph compares the nuclear/cytoplasmic ratio and the average PLK1 intensity in LP cells across 24 cases; a total number of 11,358 LP cells were analyzed. Scale bars = 20 μ m (**A**). DLBCL, diffuse large B-cell lymphoma; HGBCL, high-grade B-cell lymphoma with MYC rearrangements; PMBCL, primary mediastinal B-cell lymphoma; THRBCL, T-cell/histiocyte-rich large B-cell lymphoma.

lymphomas, in which PLK1 exhibited predominantly high-intensity nuclear intensity and decreased cytoplasmic expression (Figure 2 and Supplemental Figure S2). PLK1 expression was also evaluated in *de novo* T-cell/histiocyte-rich large B-cell lymphomas ($n = 5$). In these cases, the neoplastic cells also showed variable intense expression of PLK1 in both the nuclear and cytoplasmic compartments (Figure 2) in a pattern indistinguishable from that in the NLPHL cases. An mIF panel was performed in a subset ($n = 21$) of the NLPHL cases. The panel included markers identifying populations of CD3⁺PD1⁺ T cells, CD20⁺ B cells, and PLK1⁺ LP cells. Multiplex imaging identified LP cells surrounded by rosettes of CD3⁺/

PD1⁺ T-cell lymphocytes (Figure 2 and Supplemental Figure S3). In addition, quantitative analysis from the immunofluorescence multiplex demonstrated a linear correlation between total PLK1 staining intensity and the nuclear/cytoplasmic ratio of the PLK1 signal ($R^2 = 0.96$; $n = 11,358$) (Figure 2). This was consistent with previous studies showing increased PLK1 protein stability within the nuclear compartment compared with the cytoplasmic compartment.^{17,20,21} Overall, the findings demonstrate that PLK1 expression can be detected in LP cells in a large subset of NLPHL cases, and that higher levels of PLK1 expression correlate with increased nuclear localization.

PLK1 Expression Is Infrequent in Classic Hodgkin Lymphoma Cases

The histologic distinction between NLPHL and cHL may be problematic when LP cells co-express CD30, or when the morphologic features of Reed-Sternberg (RS) cells overlap with those of LP cells, as in the lymphocyte-rich variant of cHL. Therefore, PLK1 expression was also evaluated in a cohort of cHL cases ($n = 70$). Dual staining of PLK1/CD30 was used to detect PLK1 expression within RS cells. About 9% of the cHL cases tested included RS cells expressing PLK1 ($n = 6$) (Figure 3). In these cHL cases, the PLK1⁺ RS cells comprised <15% of total RS cells analyzed, and exhibited low, mostly cytoplasmic, expression (Figure 3). These findings suggest that PLK1 expression in cHL occurs infrequently compared with NLPHL.

PLK1 Promotes MYC Protein Expression and Tumor Growth in NLPHL

PLK1 expression correlates with increased stability of the MYC protein and adverse clinical outcomes in high-grade B-cell lymphomas.^{18,22} Therefore, MYC protein expression was evaluated in the DEV (NLPHL) cell line in the presence or absence of the selective PLK1 kinase inhibitor volasertib. DEV cells treated with volasertib showed decreased

expression of MYC protein (Figure 4). In addition, proliferation assays were performed to evaluate the contribution of PLK1 kinase activity to the growth of NLPHL tumor cells. Treatment with volasertib decreased the proliferation and increased the cell death of DEV cell lines in a dose-dependent manner and in a proportion similar to that achieved in a T-cell lymphoma cell line (MAC1) known to express PLK1 protein (Figure 4 and Supplemental Figure S4). Overall, these findings indicate that PLK1 can promote MYC protein levels and the survival of NLPHL cell lines.

PLK1 Expression Correlates with the Clinical Stage of NLPHL

Clinical data, including age at diagnosis, response to therapy, and disease stage, were available for 69 cases in the NLPHL cohort (Table 2). The median age at diagnosis was 41.2 years, and most patients were men [$n = 45$ (65%)]. Most patients (60%; $n = 42$) presented with advanced disease stage (stage 3 to 4). Initial management included radiotherapy alone [$n = 12$ (17%)], chemotherapy alone [$n = 46$ (67%)], or active surveillance [$n = 11$ (16.0%)]. The patients who received chemotherapy were treated with CHOP (cyclophosphamide, doxorubicin, vincristine, prednisolone) [$n = 24$ (52%)], ABVD (doxorubicin, bleomycin,

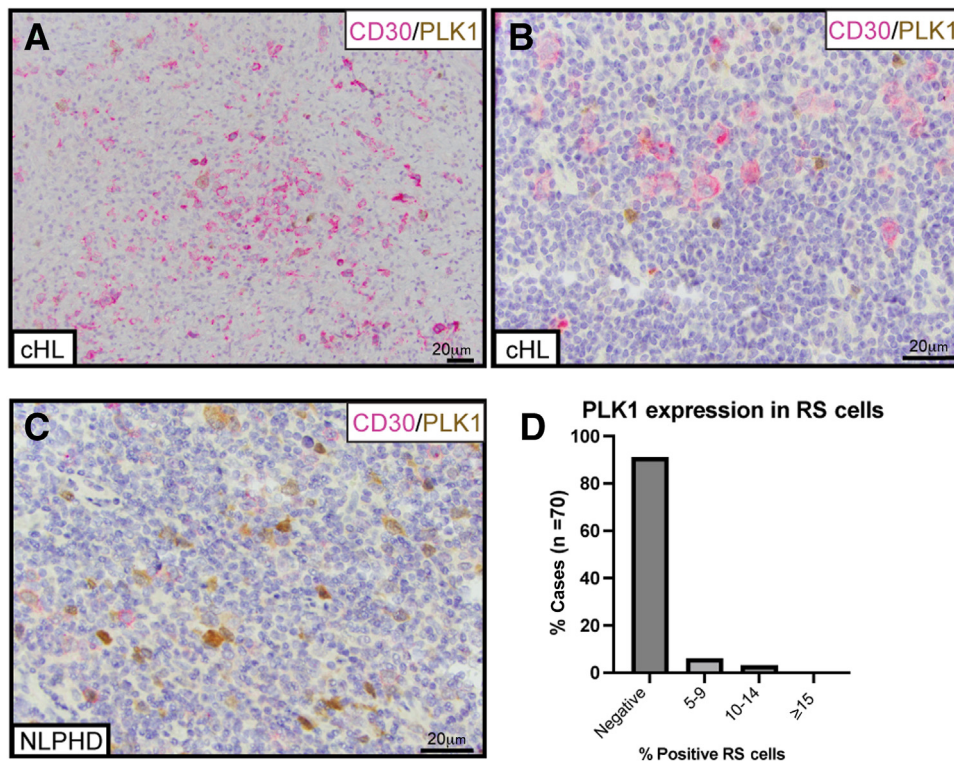


Figure 3 Polo-like kinase 1 (PLK1) expression in classic Hodgkin lymphoma (cHL) cases. **A** and **B**: cHL cases were stained for CD30 (pink) and PLK1 (brown). Reed-Sternberg (RS) cells (CD30 positive) rarely feature PLK1 expression. **C**: Nodular lymphocyte-predominant Hodgkin lymphoma (NLPHL) case stained with the same combination of markers shows few weak CD30-positive cells in the background (immunoblasts) that are negative for PLK1. **D**: Distribution of cHL cases with different percentages of PLK1-positive Reed-Sternberg cells. Scale bars = 20 μ m (A–C).

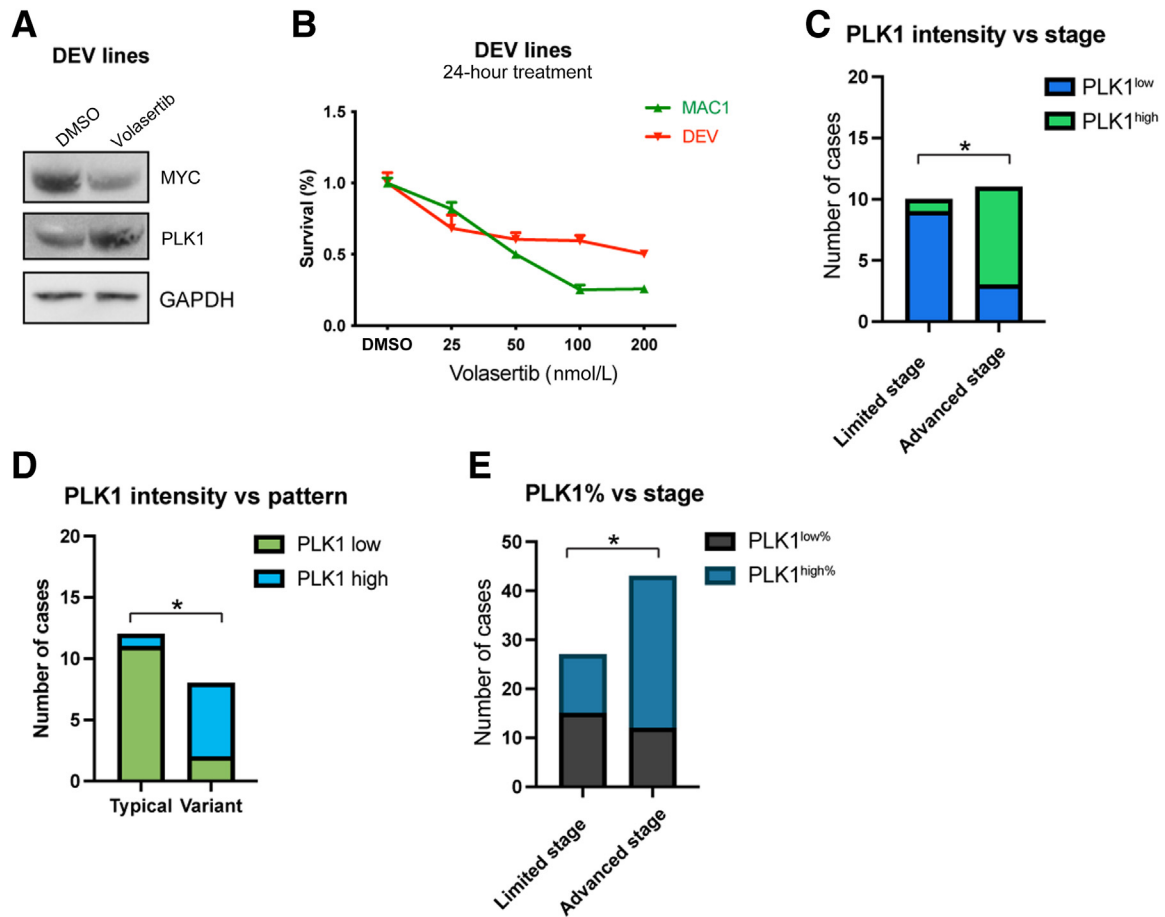


Figure 4 MYC protein expression and tumor growth in nodular lymphocyte-predominant Hodgkin lymphoma (NLPHL). **A:** DEV (NLPHL) cells were treated with 100 nmol/L of volasertib for 2 hours, and the expression levels of MYC were evaluated by Western blot analysis. **B:** Treatment of DEV and MAC1 (cutaneous T-cell lymphoma) cell lines with volasertib indicates a dose-dependent decrease in survival in 24 hours of treatment. **C:** Stacked bars indicate that cases with polo-like kinase 1 (PLK1)^{high} expression are predominantly at the advanced stage. **D:** Contingency graph indicates that cases with PLK1^{high} expression predominantly featured a variant architectural morphology. **E:** Contingency graph indicates that cases with higher PLK1-positive lymphocyte-predominant cells are predominantly at the advanced stage. * $P < 0.05$ (Fisher exact test). DMSO, dimethyl sulfoxide; GAPDH, glyceraldehyde-3-phosphate dehydrogenase.

vinblastine, dacarbazine) [$n = 14$ (30%)], or other regimens [$n = 8$ (17%)]. A small number of cases [$n = 5$ (7%)] transformed into more aggressive lymphomas. The median follow-up period was 48.2 months, and 5-year overall survival was 94%.

Kinase activity of PLK1 was associated with increased MYC protein stability and proliferation of NLPHL cell lines (Figure 4). Nuclear localization of PLK1 is required to promote MYC protein stability and entry into the cell cycle and correlates directly with increased PLK1 protein stability.^{17,21} As MYC expression is associated with tumor proliferation and aggressive behavior in B-cell lymphomas, the study sought to evaluate the correlation between the nuclear intensity of PLK1 and clinical parameters of disease progression. On the basis of the PLK1 nuclear staining detected using a multiplex immunofluorescence panel (24 cases and 11,358 LP cells analyzed) (Figure 2), a threshold was set for high or low nuclear PLK1 intensity. Subsequently, the percentage of LP cells with PLK1^{high} expression was

determined in each case, and the cases were dichotomized using a cutoff of 20%. The clinical stage at diagnosis was available for 21 of the cases analyzed, and based on this threshold, 43% of the cases featured $\geq 20\%$ LP cells with higher nuclear (not cytoplasmic) intensity PLK1 signals (PLK1^{high}). Correlation with nuclear/cytoplasmic ratio of PLK1 signal indicates that PLK1^{high} cases predominantly featured nuclear PLK1 signals (Supplemental Figure S5). Correlation with the disease stage demonstrated that 89% ($n = 9$) of these cases with $\geq 20\%$ PLK1^{high} LP cells were diagnosed at an advanced (stage 3 or 4) clinical stage (Fisher exact test, $P < 0.01$). In addition, 90% ($n = 12$) of the cases with $< 20\%$ PLK1^{high} LP cells were diagnosed at limited (stage 1 or 2) clinical stage (Fisher exact test, $P < 0.01$) (Figure 4). Variant histologic patterns (patterns C, D, E, or F of Fan et al²³) constitute an independent prognostic factor for poor outcomes in NLPHL.² Correlation between PLK1 intensity and the histologic patterns²³ demonstrated that 92% ($n = 12$) of the cases with a

Table 2 Demographics of the Patients Included in the Study

Patient demographics	Value (N = 69)
Average age, years	41.2
Stage	
I	14 (21.7)
II	13 (18.8)
III	25 (36.2)
IV	17 (24.6)
Sex	
Male	45 (65.2)
Female	24 (34.8)
Treatment	
Chemotherapy	46 (66.6)
CHOP-based regimen	24 (52.2)
ABVD regimen	14 (30.4)
Other regimen	8 (17.4)
Radiotherapy	12 (17.4)
Active surveillance	11 (15.9)
Median follow-up, months	48.2
Transformation to aggressive lymphoma	5 (7.2)
5-Year overall survival, %	94

Data are given as number (percentage) unless otherwise indicated.

ABVD, doxorubicin, bleomycin, vinblastine, dacarbazine; CHOP, cyclophosphamide, doxorubicin, vincristine, prednisolone

typical histologic pattern featured <20% of PLK1^{high} LP cells (Figure 4). Consistent with this finding, 75% (*n* = 8) of the cases with a variant histologic pattern had ≥20% PLK1^{high} LP cells (Fisher exact test, *P* < 0.01), indicating that cases with a high proportion of PLK1^{high} LP cells have variant histologic patterns.

Correlation of PLK1 expression and disease stage was performed in additional NLPHL cases not included in the set analyzed by multiplex immunofluorescence. The percentage of tumor cells with positive immunohistochemical expression of PLK1 was analyzed in 69 cases. Quantitative analysis of PLK1 staining intensity was not performed, as it varied significantly between the PLK1⁺ LP cells in each case analyzed, preventing the use of semiquantitative criteria based on light microscopy observation. On the basis of the distribution of the PLK1⁺ LP-cell percentages, a

cutoff of 80% PLK1⁺ LP cells was chosen to define cases as PLK1^{high%} or PLK1^{low%}. Using this cutoff, cases with ≥80% PLK1⁺ LP cells (PLK1^{high%}) accounted for 61% of the cases (*n* = 69). Most cases (72%; *n* = 43) associated with advanced disease stage at diagnosis had ≥80% PLK1⁺ LP cells (PLK1^{high%}, Fisher exact test, *P* < 0.01). Consistent with this, more than half of cases associated with limited-stage disease at diagnosis (56%; *n* = 26) had <80% PLK1⁺ LP cells at diagnosis (PLK1^{low%}, Fisher exact test, *P* < 0.01). The findings suggest that the percentage of PLK1⁺ LP cells correlates directly with an advanced clinical stage at diagnosis in NLPHL.

Multiplex Analysis Identifies Specific Subsets of Immune Cells within the Immediate Vicinity of LP Cells

mIF panels combined with artificial intelligence algorithms can be used to characterize the complex and dynamic composition of the tumor microenvironment. The specific expression of PLK1 within LP cells in NLPHL facilitates identifying the immediate tumor microenvironment repertoire of LP cells using these techniques. Therefore, a targeted mIF panel was performed to determine the relative frequencies of specific lymphocyte subsets in the immediate neighborhood of LP cells (three-/five-cell ratio; 40-μm radius distance) (Supplemental Figure S6). The mIF analysis identified 11,358 LP cells in 21 cases, with 1,138,160 lymphocytes (CD3⁺ or CD20⁺ cells) localized within a 40-μm radius (Table 3). The most abundant lymphocytes were T cells, accounting for 85% of the total lymphoid events. Within this T-cell fraction, T-helper type (CD3⁺/CD4⁺) lymphocytes and cytotoxic T cells (CD3⁺/CD8⁺) comprised 48% and 32% of events, respectively. T-cell follicular helper-type (CD3⁺/CD4⁺/PD1^{high+}/FoxP3⁻) cells comprised 1% of the total lymphocytes, and T-regs (CD3⁺/CD4⁺/CD8⁻/FoxP3⁺) represented <1% of the T-helper type lymphocytes. In addition, double-positive CD4/CD8 populations were detected in nearly all cases, accounting for 12% of total T cells (Table 3).

Table 3 Percentage and Total Number of Lymphocyte Subsets Identified Near LP Cells (40-μm Radius)

Lymphocyte subset	Immunophenotype	Total number of lymphocyte subsets	% of Lymphocyte subsets
B cells	CD20 ⁺ , CD3 ⁺	140,611	15
T cells	CD3 ⁺ , CD20 ⁻	767,933	85
Double positive, T cells	CD3 ⁺ , CD4 ⁺ , CD8 ⁺	109,228	12
Cytotoxic T cells	CD3 ⁺ , CD4 ⁻ , CD8 ⁺	247,512	27
Helper type, T cells	CD3 ⁺ , CD4 ⁺ , CD8 ⁻	431,793	48
Follicular helper, T cells	CD3 ⁺ , CD4 ⁺ , CD8 ⁻ , PD1 ^{high}	5798	1
Regulatory, T cells	CD3 ⁺ , CD4 ⁺ , CD8 ⁻ , FoxP3 ⁺	288	<1

A total of 11,358 LP cells were analyzed across 21 cases.

FoxP3, forkhead box P3; LP, lymphocyte predominant; PD1, programmed cell death 1.

Different Frequencies of Immune Cells Are Differentially Detected According to PLK1 Levels in LP Cells

The current findings indicate that the degree of nuclear PLK1 expression correlates with the clinical disease stage and NLPHL proliferation. Therefore, the relative frequencies of different subsets of T cells in the neighborhood of LP cells with low or high PLK1 intensity (PLK1^{high} and PLK1^{low}) were determined. Among the different T-cell subtypes, T-regs are characterized by the expression of the transcription factor FoxP3 and suppressive activity against the B-cell proliferation.^{24–27} Consistent with this, an increased frequency of T-regs within a given B-cell lymphoma constitutes a favorable prognostic factor.²⁴ Compared with benign reactive lymphoid tissue, the frequency of T-regs is decreased in NLPHL cases,²⁸ suggesting a regulatory role of this group of T-cell lymphocytes in NLPHL. The present analysis demonstrated that CD4⁺ T-regulatory type T cells (CD4⁺FoxP3⁺) were more frequently detected close to PLK1^{high} LP cells [log₂ odds ratio (OR), 3.1; CI, 67%–95%; Fisher exact test, $P < 0.001$] (Figure 5 and Table 4). In addition, a specific subset of T-regs exhibits a high-level expression of PD1. This group of T-regs (follicular regulatory T cells) can suppress the expansion of T_{FH} lymphocytes and germinal center B cells.²⁹ The follicular regulatory T-cell subset accounted for approximately 5% of the T-regs and was more frequently detected in the proximity of PLK1^{high} LP cells; however, this difference did not show statistical significance (log₂ OR, 4.41; CI, 44%–95%; Fisher exact test, $P = 0.02$) (Figure 5 and Table 4).

Seminal studies have demonstrated the anti-tumor role of cytotoxic CD8⁺ T-cell lymphocytes in lymphoid malignancies.³⁰ The degree of cytotoxic CD8⁺ T-cell tumor infiltration correlates inversely with advanced tumor stage and poor prognosis in solid tumors and B-cell lymphomas, including NLPHL.^{9,31–34} Analysis of the mIF findings indicated that the frequency of cytotoxic T cells was increased in proximity to PLK1^{high} LP cells (log₂ OR, 0.76; $P < 0.05$) (Figure 5 and Table 4). Notably, the cytotoxic activity of CD8⁺ T cells can be abrogated by persistent antigenic exposure, which correlates with the surface expression of the co-inhibitory receptors hepatitis A virus cellular receptor 2 (HAVCR2, alias TIM-3), lymphocyte activating 3 (LAG-3), and PD1.^{35,36} Therefore, the frequency and localization of these dysfunctional CD8⁺ T cells³⁶ were also evaluated in the NLPHL cases. The results demonstrate that cytotoxic T cells co-expressing TIM-3 and PD1 were nearly absent in the immediate vicinity of most LP cells and accounted for <0.001% of the total CD8 T-cell lymphocytes. The frequencies of additional subsets of cytotoxic T cells were also analyzed. Subsets of cytotoxic T cells co-expressing PD1 or FoXP3 (and negative for markers of exhaustion; eg, TIM-3) have been described as enriched in solid tumors. The significance of this group of

cytotoxic cells remains to be established, as anti-tumor or protumor effects have been described.^{35,37–42} In the present NLPHL cases, the subset of PD1⁺/TIM-3[–] cytotoxic T cells and FoxP3⁺/TIM-3[–] CD8⁺ T cells appeared at higher frequencies in the vicinity of PLK1^{high} LP cells (Figure 5).

T-helper type T cells liaise with B-cell lymphocytes, induce bacteria killing, and coordinate immune responses against helminths.^{43–46} A subset of T-helper lymphocytes called T_{FH} lymphocytes co-expresses the chemokine receptor C-X-C motif chemokine receptor 5 (CXCR5) and the immune checkpoint protein PD1 and exhibits a unique gene-expression profile.^{47–50} T_{FH} lymphocytes provide CD40 ligands to germinal center B cells, an interaction required for B-cell lymphocyte survival and differentiation.^{51,52} T_{FH} lymphocytes can be identified by their high expression level of PD1 (PD1^{high}). However, a subset of T_{FH} lymphocytes expressing PD1 at relatively low levels (PD1^{low}), co-expressing the co-inhibitory receptor TIM-3, is considered to represent an exhausted T_{FH} subset.⁵³ The spatial proximity between T_{FH} lymphocytes and marginal zone lymphoma cells correlates directly with increased proliferation rates of the lymphoma cells.⁵⁴ In addition, the increased frequency of PD1^{low} exhausted T_{FH} lymphocytes^{53,54} is associated with a worse prognosis in follicular lymphoma and diffuse large B-cell lymphoma.⁵³ Analysis of the differential frequencies of T_{FH} pools in the present NLPHL cases did not demonstrate a substantial increase in the frequency of T-helper PD1^{high} lymphocytes in proximity to PLK1^{high} LP cells (log₂ OR, 0.37) (Figure 5 and Table 4). In addition, the subset of PD1^{low} TIM3⁺ T_{FH} lymphocytes represented <0.001% of the total T cells, and no significant differences were observed in the frequency of occurrence of these cells near PLK1^{high} or PLK1^{low} LP cells.

Discussion

In contrast to that in small B-cell lymphomas, the high frequency of expression of PLK1 in NLPHL indicates that up-regulated PLK1 expression may be specific to subsets of lymphoma cells with distinct nuclear structure abnormalities.^{12,55} Similar to aggressive B-cell counterparts, in NLPHL, the kinase activity of PLK1 can promote the stability of MYC protein in NLPHL. In addition, the increased nuclear staining intensity of PLK1 occurs predominantly in NLPHL cases with variant histologic morphologies. These variants represent intermediate stages between NLPHL with typical architectural patterns and transformation into aggressive counterparts.^{12,56,57} Therefore, dysregulation of epigenetic mechanisms that mediate the nuclear translocation of PLK1, such as sumoylation,^{20,22} may contribute to the transformation and progression of NLPHL to aggressive forms. Consistent with prior studies, these findings support the driver role of MYC during the growth and expansion of NLPHL.⁹ This suggests a potential role for

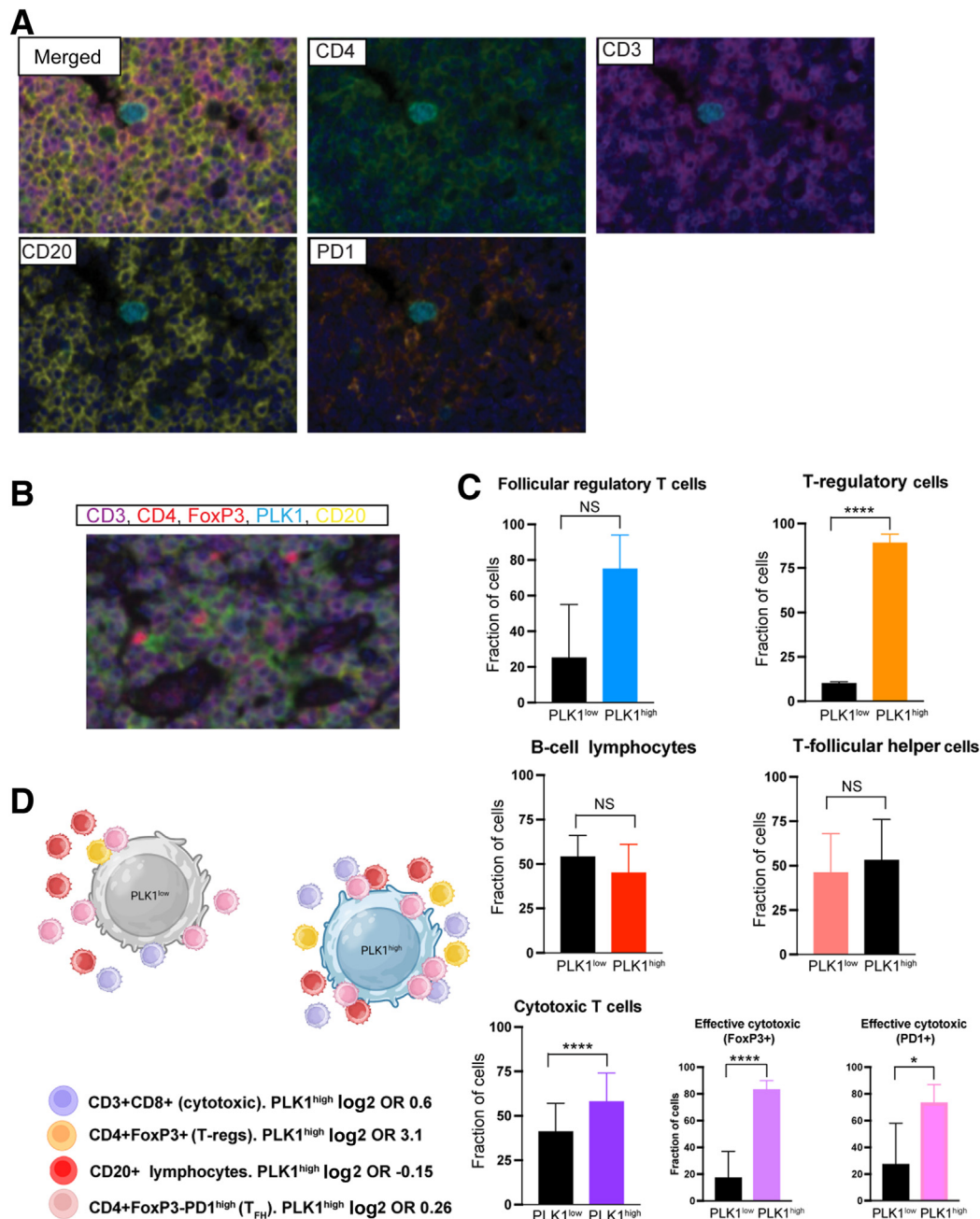


Figure 5 Multiplex immunofluorescence imaging analysis of nodular lymphocyte-predominant Hodgkin lymphoma cases highlights a different subset of immune tumor microenvironment elements in the vicinity of lymphocyte-predominant (LP) cells [polo-like kinase 1 (PLK1) positive]. **A:** Representative images of the frequently identified lymphocytes located in the vicinity of LP cells. **B:** Representative images to highlight TIM-3–positive T-cell subsets. **C:** Graphical representation of the fraction of subsets of lymphocyte populations differentially identified near LP cells with PLK1^{low} or PLK1^{high} expression. **D:** Graphical representation of the distinct lymphocytic populations enriched in proximity to LP cells. * $P < 0.05$, **** $P < 0.0001$. FoxP3, forkhead box P3; NS, nonsignificant; OR, odds ratio; T_{FH}, T-follicular helper; T-reg, T-regulatory cell.

evaluating PLK1 staining intensity and percentage positivity as a prognostic marker in NLPHL cases, as higher PLK1 expression levels correlate with advanced disease stage. In addition, on average, patients who transformed to diffuse large B-cell lymphoma had higher expression PLK1 levels at diagnosis than those that did not transform to more aggressive lymphoma. However, these findings were not statistically significant, possibly because of the relatively

small number of transformed patients in this cohort ($n = 5$). These results support the role of PLK1 in clinical disease progression and transformation. Although most patients with NLPHL have favorable outcomes, the subset with more aggressive disease may benefit from combination therapies, including selective PLK1 inhibitors. However, larger patient cohorts will be necessary for more definitive conclusions.

Table 4 Frequencies of T-Cell Subsets Near (40- μ m Radius) LP Cells

T-cell subsets	Immunophenotype	Total no.		Log ₂ OR	Fraction, % PLK1 ^{high}	CI log ₂ OR, %		P value	Significance
		PLK1 ^{high}	PLK1 ^{low}			Fraction, % PLK1 ^{high}	Fraction, % PLK1 ^{low}		
T-regs	CD3 ⁺ , CD4 ⁺ , FoxP3 ⁺ , PD1 ^{low/neg}	240	29	3.1	90	67–95	10	5–10	0.000001 ****
Follicular regulatory T cells	CD3 ⁺ , CD4 ⁺ , FoxP3 ⁺ , PD1 ^{high}	14	5	1.5	73	42–93	26	6–57	0.150000 NS
Cytotoxic T cells	CD3 ⁺ , CD8 ⁺	152,023	95,489	0.7	61	42–75	38	24–57	0.000200 ****
Dysfunctional cytotoxic T cells	CD3 ⁺ , CD8 ⁺ , TIM-3 ⁺ , PD1 ⁺	44	12	1.9	78	37–93	21	6–62	0.070000 NS
Subset effective cytotoxic T cells	CD3 ⁺ , CD8 ⁺ , PD1 ⁺ , TIM-3 ⁻	20,405	7528	1.5	73	42–87	27	12–58	0.010000 *
Subset effective cytotoxic T cells	CD3 ⁺ , CD8 ⁺ , FoxP3 ⁺	1959	410	2.3	83	62–90	17	9–37	0.000001 ****
T-follicular helper cells	CD3 ⁺ , CD4 ⁺ , FoxP3 ⁻ , PD1 ^{high}	3242	2556	0.3	55	31–82	44	17–68	0.550000 NS
Exhausted T-follicular helper cells	CD3 ⁺ , CD4 ⁺ , FoxP3 ⁻ , PD1 ^{low} , TIM-3 ⁺	104	12	0.8	41	41–82	36	17–58	0.120000 NS
Double CD4/CD8 positive T cells	CD3 ⁺ , CD4 ⁺ , CD8 ⁺	65,887	43,341	0.6	60	42–77	40	22–58	0.030000 NS
B-cell lymphocytes	CD20 ⁺	66,683	73,928	-0.1	47	33–64	52	35–66	1.3 NS

The fraction and CI of each subset identified close to LP cells with PLK1^{high} and PLK1^{low} intensities are indicated.

* $P < 0.05$, **** $P < 0.0001$.

FoxP3, forkhead box P3; LP, lymphocyte predominant; PD1, programmed cell death 1; NS, nonsignificant statistical difference; OR, odds ratio; PLK1, polo-like kinase 1; T-reg, T-regulatory cell.

The findings demonstrate that the characteristic cytoplasmic and nuclear expression of PLK1 in LP cells is distinct from that of more aggressive B-cell lymphomas that commonly feature a strong and predominantly nuclear expression of PLK1. T-cell/histiocyte-rich large B-cell lymphomas typically have a relatively low percentage of tumor cells (often <5%) and architectural features that mimic a subset of NLPHL cases (NLPHL pattern E). The current cohort also included three NLPHL cases with a THRLBCL-like pattern (pattern E) at relapse, and the LP cells of these cases were positive for PLK1. Moreover, the five *de novo* THRLBCL cases included herein showed positive expression of PLK1 in a variable number of tumor cells in a similar pattern as LP cells and distinct from aggressive large B-cell lymphomas (Figure 2). Similar to THRLBCL, the findings also confirmed that the tumor microenvironment of advanced-stage NLPHL comprises predominantly cytotoxic T cells.^{12,14,58} These findings support previous studies suggesting that THRLBCL and NLPHL (pattern E) cases lie along a single disease spectrum and do not represent distinct clinical entities.⁵⁸

Another notable finding is the near absence of PLK1 expression in the tumor cells of classic Hodgkin lymphoma cases. Fewer than 15% of RS cells were positive for PLK1 in rare exceptions. In contrast, most NLPHL cases in this study ($n = 76$) showed 68% PLK1⁺ LP cells on average, and no single case had <10%. Therefore, PLK1 expression

may help distinguish between cHL and NLPHL in difficult cases with atypical CD30 and B-cell antigen expression patterns, combined with other markers, such as STAT6.⁵⁹ PLK1 expression in normal lymphoid tissue occurs predominantly in germinal center lymphocytes, and CD30⁺ immunoblasts are negative for PLK1 (Figure 3). Consequently, analysis of PLK1 expression may also aid the evaluation of small biopsy specimens containing suspicious atypical, large lymphocytes.

The cytotoxic host response is a predominant feature in NLPHL cases with transformation into aggressive forms.⁹ The current multiplex immunofluorescence analysis demonstrated an increased frequency of cytotoxic T cells that correlated directly with the proliferation rate (PLK1^{high}) of LP cells. This suggests that a cytotoxic host response persists despite NLPHL-mediated immune evasion. However, these findings are limited to the characterization of immune cells in the immediate vicinity of LP cells. Also, we did not identify different frequencies of cytotoxic T cells when the cases were dichotomized by clinical stage (limited or advanced) or when differentially evaluated in cases with variant histologic patterns. This could be secondary to the limited number of cases analyzed by multiplex immunofluorescence panels. Therefore, further studies with larger case series are required to define more complex immune cell frequency distribution patterns. Expression of FoxP3 within cytotoxic T cells has been associated with potent anti-tumor

effects, as FoxP3 facilitates adaptation by helping to efficiently use glucose to maintain effector cytotoxic functions.⁶⁰ However, knockout expression of FoxP3 within cytotoxic T cells demonstrated improved anti-tumor functions in models of adoptive T-cell therapy.⁴⁰ The current findings demonstrated an increased frequency of FoxP3⁺/CD8⁺ T cells in the neighborhood of PLK1^{high} LP cells. The significance of this finding remains to be established, as the function of this subset of effector cytotoxic T cells during tumor responses has yet to be delineated. More important, the frequency of exhausted T-helper cells and cytotoxic T cells was not increased in the vicinity of LP cells with PLK1^{high} intensities; in fact, both populations were nearly absent in NLPHL cases. In addition, the relatively increased frequency of T-regs around PLK1^{high} LP cells supports a disease model in which the immunosurveillance role of T-regs is preserved.

Consistent with previous studies,¹⁶ T_{FH}-type lymphocytes were detected frequently near LP cells. The oncogenic advantage provided by T_{FH} lymphocytes during the growth of NLPHL has been described previously.¹⁶ The frequency of T_{FH} subsets was not increased near LP cells with a high proliferation rate (PLK1^{high}), which could be secondary to the increased frequency of immunomodulatory cells (such as T-regs) near the PLK1^{high} tumor cells. This finding suggests that LP cells have relatively limited control over the immediate immune surveillance program, which may explain the lower relapse rates and decreased rate of progression of NLPHL compared with aggressive B-cell lymphomas. Because PD-L1 expression occurs in 75% of NLPHL cases,⁶¹ and effector T cells predominate in the tumor microenvironment in low- and high-stage disease and in NLPHL cases with transformation into diffuse large B-cell lymphoma,⁹ the therapeutic use of immune checkpoint inhibitors could be a viable strategy for treating NLPHL⁶² at advanced stages.

Author Contributions

C.M.-Z., K.I., R.A.W., and J.W. conceived and designed the study; J.W., M.M.-C., E.B., M.S., R.A.W., K.I., and C.M.-Z. developed methods and wrote, reviewed, and revised the manuscript; J.W., V.E., V.P.-S., A.Z., M.M.-C., E.B., R.P., R.A.W., K.I., P.H.G., and C.M.-Z. acquired, analyzed, and interpreted data; and J.K.F., J.W., K.G., V.E., V.P.-S., A.Z., M.M.-C., E.B., M.S., E.S., R.P., N.L.-H., J.B., J.R., G.V., N.B., N.A.B., M.L.X., R.A.W., K.I., and C.M.Z. provided technical and material support. All authors read and approved the final manuscript.

Disclosure Statement

M.L.X. receives financial support for consultancy at Tree-line Biosciences.

Supplemental Data

Supplemental material for this article can be found at <http://doi.org/10.1016/j.ajpath.2023.10.008>.

References

- Eichenauer DA, Plutschow A, Fuchs M, von Tresckow B, Boll B, Behringer K, Diehl V, Eich HT, Borchmann P, Engert A: Long-term course of patients with stage IA nodular lymphocyte-predominant Hodgkin lymphoma: a report from the German Hodgkin Study Group. *J Clin Oncol* 2015, 33:2857–2862
- Hartmann S, Eichenauer DA, Plutschow A, Mottok A, Bob R, Koch K, Bernd HW, Cogliatti S, Hummel M, Feller AC, Ott G, Moller P, Rosenwald A, Stein H, Hansmann ML, Engert A, Klapper W: The prognostic impact of variant histology in nodular lymphocyte-predominant Hodgkin lymphoma: a report from the German Hodgkin Study Group (GHSg). *Blood* 2013, 122:4246–4252. quiz 4292
- Lazarovici J, Dartigues P, Brice P, Oberic L, Gaillard I, Hunault-Berger M, Broussais-Guillaumot F, Gyan E, Bologna S, Nicolas-Virelizier E, Touati M, Casasnovas O, Delarue R, Orsini-Piocelle F, Stamatoullas A, Gabarre J, Fornecker LM, Gastinne T, Peyrade F, Roland V, Bachy E, Andre M, Mounier N, Ferme C: Nodular lymphocyte predominant Hodgkin lymphoma: a Lymphoma Study Association retrospective study. *Haematologica* 2015, 100:1579–1586
- Xing KH, Connors JM, Lai A, Al-Mansour M, Sehn LH, Villa D, Klasa R, Shenkier T, Gascoyne RD, Skinnider B, Savage KJ: Advanced-stage nodular lymphocyte predominant Hodgkin lymphoma compared with classical Hodgkin lymphoma: a matched pair outcome analysis. *Blood* 2014, 123:3567–3573
- Kenderian SS, Habermann TM, Macon WR, Ristow KM, Ansell SM, Colgan JP, Johnston PB, Inwards DJ, Markovic SN, Micallef IN, Thompson CA, Porrata LF, Martenson JA, Witzig TE, Nowakowski GS: Large B-cell transformation in nodular lymphocyte-predominant Hodgkin lymphoma: 40-year experience from a single institution. *Blood* 2016, 127:1960–1966
- Fanale MA, Cheah CY, Rich A, Medeiros LJ, Lai CM, Oki Y, Romaguera JE, Fayad LE, Hagemister FB, Samaniego F, Rodriguez MA, Neelapu SS, Lee HJ, Nastoupil L, Fowler NH, Turturro F, Westin JR, Wang ML, McLaughlin P, Pinnix CC, Milgrom SA, Dabaja B, Horowitz SB, Younes A: Encouraging activity for R-CHOP in advanced stage nodular lymphocyte-predominant Hodgkin lymphoma. *Blood* 2017, 130:472–477
- Borchmann S, Joffe E, Moskowitz CH, Zelenetz AD, Noy A, Portlock CS, Gerecitano JF, Batlevi CL, Caron PC, Drullinsky P, Hamilton A, Hamlin PA Jr, Horwitz SM, Kumar A, Matasar MJ, Moskowitz AJ, Owens CN, Palomba ML, Younes A, Straus DJ: Active surveillance for nodular lymphocyte-predominant Hodgkin lymphoma. *Blood* 2019, 133:2121–2129
- Shet T, Panjwani P, Epari S, Sengar M, Prasad M, Arora B, Laskar S, Gujral S, Menon H, Banavali S: A simplified scoring system to document variant patterns in nodular lymphocyte predominant Hodgkin lymphoma. *Leuk Lymphoma* 2015, 56:1651–1658
- Schuhmacher B, Rengstl B, Doring C, Bein J, Newrzela S, Brunnberg U, Kvasnicka HM, Vormann M, Kuppers R, Hansmann ML, Hartmann S: A strong host response and lack of MYC expression are characteristic for diffuse large B cell lymphoma transformed from nodular lymphocyte predominant Hodgkin lymphoma. *Oncotarget* 2016, 7:72197–72210
- Diehl V, Sextro M, Franklin J, Hansmann ML, Harris N, Jaffe E, Poppema S, Harris M, Franssila K, van Krieken J, Marafioti T, Anagnostopoulos I, Stein H: Clinical presentation, course, and prognostic factors in lymphocyte-predominant Hodgkin's disease and lymphocyte-rich classical Hodgkin's disease: report from the

- European Task Force on Lymphoma Project on Lymphocyte-Predominant Hodgkin's Disease. *J Clin Oncol* 1999, 17:776–783
11. Younes S, Rojansky RB, Menke JR, Gratzinger D, Natkunam Y: Pitfalls in the diagnosis of nodular lymphocyte predominant Hodgkin lymphoma: variant patterns, borderlines and mimics. *Cancers (Basel)* 2021, 13:3021
 12. Sadeghi Shoreh Deli A, Scharf S, Steiner Y, Bein J, Hansmann ML, Hartmann S: 3D analyses reveal T cells with activated nuclear features in T-cell/histiocyte-rich large B-cell lymphoma. *Mod Pathol* 2022, 35:1431–1438
 13. Tousseyn T, De Wolf-Peeters C: T cell/histiocyte-rich large B-cell lymphoma: an update on its biology and classification. *Virchows Arch* 2011, 459:557–563
 14. Boudova L, Torlakovic E, Delabie J, Reimer P, Pfistner B, Wiedenmann S, Diehl V, Muller-Hermelink HK, Rudiger T: Nodular lymphocyte-predominant Hodgkin lymphoma with nodules resembling T-cell/histiocyte-rich B-cell lymphoma: differential diagnosis between nodular lymphocyte-predominant Hodgkin lymphoma and T-cell/histiocyte-rich B-cell lymphoma. *Blood* 2003, 102:3753–3758
 15. Zhao FX: Nodular lymphocyte-predominant Hodgkin lymphoma or T-cell/histiocyte rich large B-cell lymphoma: the problem in “grey zone” lymphomas. *Int J Clin Exp Pathol* 2008, 1:300–305
 16. Nathwani BN, Vornanen M, Winkelmann R, Kansal R, Doering C, Hartmann S, Hansmann ML: Intranodular clusters of activated cells with T follicular helper phenotype in nodular lymphocyte predominant Hodgkin lymphoma: a pilot study of 32 cases from Finland. *Hum Pathol* 2013, 44:1737–1746
 17. Bruinsma W, Aprelia M, Kool J, Macurek L, Lindqvist A, Medema RH: Spatial separation of Plk1 phosphorylation and activity. *Front Oncol* 2015, 5:132
 18. Murga-Zamalloa C, Polk A, Hanel W, Chowdhury P, Brown N, Hristov AC, Bailey NG, Wang T, Phillips T, Devata S, Poonen P, Gomez-Gelvez J, Inamdar KV, Wilcox RA: Polo-like-kinase 1 (PLK-1) and c-myc inhibition with the dual kinase-bromodomain inhibitor volasertib in aggressive lymphomas. *Oncotarget* 2017, 8: 114474–114480
 19. Altman DG, Bland JM: How to obtain the P value from a confidence interval. *BMJ* 2011, 343:d2304
 20. Wen D, Wu J, Wang L, Fu Z: SUMOylation promotes nuclear import and stabilization of polo-like kinase 1 to support its mitotic function. *Cell Rep* 2017, 21:2147–2159
 21. Kachaner D, Garrido D, Mehsen H, Normandin K, Lavoie H, Archambault V: Coupling of polo kinase activation to nuclear localization by a bifunctional NLS is required during mitotic entry. *Nat Commun* 2017, 8:1701
 22. Murga-Zamalloa C, Inamdar KV, Wilcox RA: The role of aurora A and polo-like kinases in high-risk lymphomas. *Blood Adv* 2019, 3: 1778–1787
 23. Fan Z, Natkunam Y, Bair E, Tibshirani R, Warnke RA: Characterization of variant patterns of nodular lymphocyte predominant Hodgkin lymphoma with immunohistologic and clinical correlation. *Am J Surg Pathol* 2003, 27:1346–1356
 24. Muenst S, Hoeller S, Dimhofer S, Tzankov A: Increased programmed death-1+ tumor-infiltrating lymphocytes in classical Hodgkin lymphoma substantiate reduced overall survival. *Hum Pathol* 2009, 40:1715–1722
 25. Carreras J, Lopez-Guillermo A, Fox BC, Colomo L, Martinez A, Roncador G, Montserrat E, Campo E, Banham AH: High numbers of tumor-infiltrating FOXP3-positive regulatory T cells are associated with improved overall survival in follicular lymphoma. *Blood* 2006, 108:2957–2964
 26. Tsakiroglou AM, Astley S, Dave M, Fergie M, Harkness E, Rosenberg A, Sperrin M, West C, Byers R, Linton K: Immune infiltrate diversity confers a good prognosis in follicular lymphoma. *Cancer Immunol Immunother* 2021, 70:3573–3585
 27. Kelley TW, Parker CJ: CD4 (+)CD25 (+)Foxp3 (+) regulatory T cells and hematologic malignancies. *Front Biosci (Schol Ed)* 2010, 2: 980–992
 28. Visser L, Rutgers B, Diepstra A, van den Berg A, Sattarzadeh A: Characterization of the microenvironment of nodular lymphocyte predominant Hodgkin lymphoma. *Int J Mol Sci* 2016, 17:2127
 29. Linterman MA, Pierson W, Lee SK, Kallies A, Kawamoto S, Rayner TF, Srivastava M, Divekar DP, Beaton L, Hogan JJ, Fagarasan S, Liston A, Smith KG, Vinuesa CG: Foxp3+ follicular regulatory T cells control the germinal center response. *Nat Med* 2011, 17:975–982
 30. Smyth MJ, Thia KY, Street SE, MacGregor D, Godfrey DI, Trapani JA: Perforin-mediated cytotoxicity is critical for surveillance of spontaneous lymphoma. *J Exp Med* 2000, 192:755–760
 31. Rimsza LM, Roberts RA, Miller TP, Unger JM, LeBlanc M, Brazier RM, Weisenberger DD, Chan WC, Muller-Hermelink HK, Jaffe ES, Gascoyne RD, Campo E, Fuchs DA, Spier CM, Fisher RI, Delabie J, Rosenwald A, Staudt LM, Grogan TM: Loss of MHC class II gene and protein expression in diffuse large B-cell lymphoma is related to decreased tumor immunosurveillance and poor patient survival regardless of other prognostic factors: a follow-up study from the Leukemia and Lymphoma Molecular Profiling Project. *Blood* 2004, 103:4251–4258
 32. Rajnai H, Heyning FH, Koens L, Sebestyen A, Andrikovics H, Hogendoorn PC, Matolcsy A, Szepesi A: The density of CD8+ T-cell infiltration and expression of BCL2 predicts outcome of primary diffuse large B-cell lymphoma of bone. *Virchows Arch* 2014, 464:229–239
 33. Shankaran V, Ikeda H, Bruce AT, White JM, Swanson PE, Old LJ, Schreiber RD: IFN γ and lymphocytes prevent primary tumour development and shape tumour immunogenicity. *Nature* 2001, 410: 1107–1111
 34. Lippman SM, Spier CM, Miller TP, Slymen DJ, Rybski JA, Grogan TM: Tumor-infiltrating T-lymphocytes in B-cell diffuse large cell lymphoma related to disease course. *Mod Pathol* 1990, 3:361–367
 35. Legat A, Speiser DE, Pircher H, Zehn D, Fuertes Marraco SA: Inhibitory receptor expression depends more dominantly on differentiation and activation than “exhaustion” of human CD8 T cells. *Front Immunol* 2013, 4:455
 36. Apetoh L, Smyth MJ, Drake CG, Abastado JP, Apte RN, Ayyoub M, et al: Consensus nomenclature for CD8(+) T cell phenotypes in cancer. *Oncoimmunology* 2015, 4:e998538
 37. Gros A, Robbins PF, Yao X, Li YF, Turcotte S, Tran E, Wunderlich JR, Mixon A, Farid S, Dudley ME, Hanada K, Almeida JR, Darko S, Douek DC, Yang JC, Rosenberg SA: PD-1 identifies the patient-specific CD8(+) tumor-reactive repertoire infiltrating human tumors. *J Clin Invest* 2014, 124:2246–2259
 38. Shafer-Weaver KA, Anderson MJ, Stagliano K, Malyguine A, Greenberg NM, Hurwitz AA: Cutting edge: tumor-specific CD8+ T cells infiltrating prostatic tumors are induced to become suppressor cells. *J Immunol* 2009, 183:4848–4852
 39. Shafer-Weaver KA, Watkins SK, Anderson MJ, Draper LJ, Malyguine A, Alvord WG, Greenberg NM, Hurwitz AA: Immunity to murine prostatic tumors: continuous provision of T-cell help prevents CD8 T-cell tolerance and activates tumor-infiltrating dendritic cells. *Cancer Res* 2009, 69:6256–6264
 40. Lozano T, Conde E, Martin-Otal C, Navarro F, Lasarte-Cia A, Nasrallah R, Alignani D, Gorraiz M, Sarobe P, Romero JP, Vilas A, Roychoudhuri R, Hervas-Stubbs S, Casares N, Lasarte JJ: TCR-induced FOXP3 expression by CD8(+) T cells impairs their anti-tumor activity. *Cancer Lett* 2022, 528:45–58
 41. Mishra S, Srinivasan S, Ma C, Zhang N: CD8(+) regulatory T cell - a mystery to be revealed. *Front Immunol* 2021, 12:708874
 42. Le DT, Ladle BH, Lee T, Weiss V, Yao X, Leubner A, Armstrong TD, Jaffee EM: CD8(+) Foxp3(+) tumor infiltrating lymphocytes accumulate in the context of an effective anti-tumor response. *Int J Cancer* 2011, 129:636–647
 43. Noelle RJ, Roy M, Shepherd DM, Stamenkovic I, Ledbetter JA, Aruffo A: A 39-kDa protein on activated helper T cells binds CD40 and transduces the signal for cognate activation of B cells. *Proc Natl Acad Sci U S A* 1992, 89:6550–6554

44. Vinuesa CG, Linterman MA, Yu D, MacLennan IC: Follicular helper T cells. *Annu Rev Immunol* 2016, 34:335–368
45. Kaplan MH, Whitfield JR, Boros DL, Grusby MJ: Th2 cells are required for the *Schistosoma mansoni* egg-induced granulomatous response. *J Immunol* 1998, 160:1850–1856
46. Cooper AM, Dalton DK, Stewart TA, Griffin JP, Russell DG, Orme IM: Disseminated tuberculosis in interferon gamma gene-disrupted mice. *J Exp Med* 1993, 178:2243–2247
47. Chtanova T, Tangye SG, Newton R, Frank N, Hodge MR, Rolph MS, Mackay CR: T follicular helper cells express a distinctive transcriptional profile, reflecting their role as non-Th1/Th2 effector cells that provide help for B cells. *J Immunol* 2004, 173:68–78
48. Kim CH, Lim HW, Kim JR, Rott L, Hillsamer P, Butcher EC: Unique gene expression program of human germinal center T helper cells. *Blood* 2004, 104:1952–1960
49. Dorfman DM, Brown JA, Shahsafaie A, Freeman GJ: Programmed death-1 (PD-1) is a marker of germinal center-associated T cells and angioimmunoblastic T-cell lymphoma. *Am J Surg Pathol* 2006, 30:802–810
50. Haynes NM, Allen CD, Lesley R, Ansel KM, Killeen N, Cyster JG: Role of CXCR5 and CCR7 in follicular Th cell positioning and appearance of a programmed cell death gene-1-high germinal center-associated subpopulation. *J Immunol* 2007, 179:5099–5108
51. Liu YJ, Joshua DE, Williams GT, Smith CA, Gordon J, MacLennan IC: Mechanism of antigen-driven selection in germinal centres. *Nature* 1989, 342:929–931
52. Arpin C, Dechanet J, Van Kooten C, Merville P, Grouard G, Briere F, Banchereau J, Liu YJ: Generation of memory B cells and plasma cells in vitro. *Science* 1995, 268:720–722
53. Yang ZZ, Grote DM, Ziesmer SC, Xiu B, Novak AJ, Ansell SM: PD-1 expression defines two distinct T-cell sub-populations in follicular lymphoma that differentially impact patient survival. *Blood Cancer J* 2015, 5:e281
54. Wickenden K, Nawaz N, Mamand S, Kotecha D, Wilson AL, Wagner SD, Ahearn MJ: PD1(hi) cells associate with clusters of proliferating B-cells in marginal zone lymphoma. *Diagn Pathol* 2018, 13:74
55. Zink D, Fischer AH, Nickerson JA: Nuclear structure in cancer cells. *Nat Rev Cancer* 2004, 4:677–687
56. Schuhmacher B, Bein J, Rausch T, Benes V, Tousseyn T, Vornanen M, Ponzoni M, Thurner L, Gascoyne R, Steidl C, Kuppers R, Hansmann ML, Hartmann S: JUNB, DUSP2, SGK1, SOCS1 and CREBBP are frequently mutated in T-cell/histiocyte-rich large B-cell lymphoma. *Haematologica* 2019, 104:330–337
57. Hartmann S, Doring C, Vucic E, Chan FC, Ennishi D, Tousseyn T, de Wolf-Peters C, Perner S, Wlodarska I, Steidl C, Gascoyne RD, Hansmann ML: Array comparative genomic hybridization reveals similarities between nodular lymphocyte predominant Hodgkin lymphoma and T cell/histiocyte rich large B cell lymphoma. *Br J Haematol* 2015, 169:415–422
58. Hartmann S, Doring C, Jakobus C, Rengstl B, Newrzela S, Tousseyn T, Sagaert X, Ponzoni M, Facchetti F, de Wolf-Peters C, Steidl C, Gascoyne R, Kuppers R, Hansmann ML: Nodular lymphocyte predominant Hodgkin lymphoma and T cell/histiocyte rich large B cell lymphoma—endpoints of a spectrum of one disease? *PLoS One* 2013, 8:e78812
59. Van Slambrouck C, Huh J, Suh C, Song JY, Menon MP, Sohani AR, Duffield AS, Goldberg RC, Dama P, Kiyotani K, Godfrey J, Fitzpatrick C, Kline J, Smith SM, Jaffe ES, Hartmann S, Venkataraman G: Diagnostic utility of STAT6(YE361) expression in classical Hodgkin lymphoma and related entities. *Mod Pathol* 2020, 33:834–845
60. Conde E, Casares N, Mancheno U, Elizalde E, Vercher E, Capozzi R, Santamaria E, Rodriguez-Madoz JR, Prosper F, Lasarte JJ, Lozano T, Hervas-Stubbs S: FOXP3 expression diversifies the metabolic capacity and enhances the efficacy of CD8 T cells in adoptive immunotherapy of melanoma. *Mol Ther* 2023, 31:48–65
61. Panjwani PK, Charu V, DeLisser M, Molina-Kirsch H, Natkunam Y, Zhao S: Programmed death-1 ligands PD-L1 and PD-L2 show distinctive and restricted patterns of expression in lymphoma subtypes. *Hum Pathol* 2018, 71:91–99
62. Ansell SM, Lesokhin AM, Borrello I, Halwani A, Scott EC, Gutierrez M, Schuster SJ, Millenson MM, Cattray D, Freeman GJ, Rodig SJ, Chapuy B, Ligon AH, Zhu L, Grosse JF, Kim SY, Timmerman JM, Shipp MA, Armand P: PD-1 blockade with nivolumab in relapsed or refractory Hodgkin's lymphoma. *N Engl J Med* 2015, 372:311–319